PCCP

PAPER

View Article Online
View Journal



Cite this: DOI: 10.1039/c8cp02352b

# Successive C1–C2 bond cleavage: the mechanism of vanadium(v)-catalyzed aerobic oxidation of D-glucose to formic acid in aqueous solution†

Muge Niu,[a] Yucui Hou,[b] Weize Wu,*[a] Shuhang Ren[a] and Ru Yang[c]

Vanadium(v)-catalyzed aerobic oxidation in aqueous solution shows high selectivity in the field of C–C bond cleavage of carbohydrates for chemicals with less carbon atoms. However, the pathway of C–C bond cleavage from carbohydrates and the conversion mechanism are unclear. In this work, we studied the pathway and the mechanism of D-glucose oxidation to formic acid (FA) in $NaVO_3$–$H_2SO_4$ aqueous solution using isotope-labeled glucoses as substrates. D-Glucose is first transformed to FA and D-arabinose *via* C1–C2 bond cleavage. D-Arabinose undergoes similar C1–C2 bond cleavage to form FA and the corresponding D-erythrose, which can be further degraded by C1–C2 bond cleavage. Dimerization and aldol condensation between carbohydrates can also proceed to make the reaction a much more complicated mixture. However, the fundamental reaction, C1–C2 bond cleavage, can drive all the intermediates to form the common product FA. Based on the detected intermediates, isotope-labelling experiments, the kinetic isotope effect study and kinetic analysis, this mechanism is proposed. D-Glucose first reacts with a vanadium(v) species to form a five-membered-ring complex. Then, electron transfer occurs and the C1–C2 bond weakens, followed by C1–C2 bond cleavage (with no C–H bond cleavage), to generate the $H_3COO^{\bullet}$–vanadium(iv) complex and D-arabinose. FA is generated from $H_3COO^{\bullet}$ that is oxidized by another vanadium(v) species. The reduced vanadium species is oxidized by $O_2$ to regenerate to its oxidation state. This finding will provide a deeper insight into the process of C–C bond cleavage of carbohydrates for chemical synthesis and provide guidance for screening and synthesizing new highly-efficient catalyst systems for FA production.

Received 13th April 2018,
Accepted 1st June 2018

DOI: 10.1039/c8cp02352b

rsc.li/pccp



## 1. Introduction

Selective conversion of sufficient renewable bio-derived carbohydrates into chemicals shows great potential as an alternative strategy for solving problems caused by fossil fuel utilization. Compared with widely used biochemical processes, catalysis often provides more options for the tunable design of products.[1–3] Highly selective catalytic routes for chemicals from carbohydrates have been developed for decades. Representative successful examples are Lewis acid-catalyzed isomerization/dehydration of D-glucose to yield 5-hydroxymethyl furfural, and metal-catalyzed C–H bond activation to yield the corresponding sugar acids and sugar alcohols.

Notably, for value-added products with less carbon atoms from carbohydrates, selective C–C bond cleavage is required. However, the C–C bond cleavage of carbohydrates often exhibits various byproducts or requires harsh conditions, even in some current effective catalytic processes. For example, 3–11% byproduct formation in methyl lactate production from glucose and sucrose occurs in methanol catalyzed by Lewis acidic zeolites.[4] Various kinds of alcohols are generated in ethylene glycol production from cellulose and glucose *via* tungsten carbide/oxide-catalyzed hydrogenation.[5–7] High temperature and an excess amount of alkali were required while producing C1–C3 products with high yields *via* oxidation.[8–11]

The low efficiency of C–C bond cleavage of carbohydrates is possibly attributed to two reasons. First, the high steric constraints derived from each carbon atom bonded to a hydrogen atom and a hydroxyl group make the catalyst hard to approach. Second, various reactions easily occur in carbohydrate solution, including tautomerism, dehydration, rearrangement acetalization and aldol/retro-aldol condensation,[12]

[a] State Key Laboratory of Chemical Resource Engineering, College of Chemical Engineering, Beijing University of Chemical Technology, Beijing 100029, P. R. China. E-mail: wzwu@mail.buct.edu.cn; Fax: +86 10 64427603; Tel: +86 10 64427603
[b] Department of Chemistry, Taiyuan Normal University, Taiyuan 030031, P. R. China
[c] College of Materials Science and Engineering, Beijing University of Chemical Technology, 100029, Beijing, P. R. China

† Electronic supplementary information (ESI) available: Schemes S1 and S2, and Fig. S1–S12. See DOI: 10.1039/c8cp02352b

leading to competition with or interference in catalytic C–C bond cleavage.

Stoichiometric inorganic high-valence oxidants (Cr(VI),[13] I(VII),[14,15] Mn(IV),[16] and Pb(IV)[17]) have long been used as reagents for C–C bond cleavage of compounds with vicinal diols to produce the corresponding carbonyl compounds. The high selectivity of C–C bond cleavage was due to the strong interaction with the adjacent hydroxyl groups to counteract the effect of steric constraints and side reactions. However, these extremely strong oxidants can hardly be recovered (by oxidation) after the reaction, leading to excess consumption and severe waste pollution.

In this context, vanadium(V) species exhibit a similar manner to the stoichiometric oxidants with a milder oxidation capacity, and thus can be used in catalytic amounts with oxygen as an oxidant.[18] Therefore, a series of homogeneous vanadium(V)-catalyzed aerobic oxidations ($H_5PV_2Mo_{10}O_{40}$,[19–26] $H_4PVMo_{11}O_{40}$,[27] $PVMo_{11}O_{40}^{4-}$-based ionic liquid,[28] $VOSO_4$[29] and $NaVO_3$–$H_2SO_4$[30–32]) were developed and significantly enhanced the selectivity of C–C bond cleavage of carbohydrates. The solvent is water and the product in the aqueous phase is solely formic acid (FA), with yields up to ~68% at 70–160 °C (the other product is $CO_2$). FA is an important chemical in industry, especially for very recent applications in hydrogen storage[33–37] and fuel cells.[38–40] Therefore, this brand new highly selective C–C bond cleavage is considered as a promising method for the production of value-added small molecular chemicals from bio-derived carbohydrates.

Fruitful results have been achieved with respect to the mechanism. Fu *et al.*[23] and Wu *et al.*[30] selected possible intermediates as substrates, and proposed a pathway from D-glucose (representative carbohydrate) to FA initiated with C2–C3 and/or C3–C4 bond cleavage *via* retro-aldol condensation, followed by continued C–C bond cleavage to form FA. Wasserscheid *et al.*[19] and Wang *et al.*[29] abstracted representative structures from D-glucose to study the transformation of each functional group. Neumann *et al.*[26] tested the product distributions of each carbon atom in D-glucose, and showed that C1 and C5 have the highest selectivity to FA and $CO_2$, respectively. Tomishige *et al.*[41] proposed a mechanism between ketol and vanadium(V) ligands under $O_2$ oxidation with a ketol–vanadium(V)–biradical $O_2$ complex as the key intermediate before C–C bond cleavage.

However, the mechanism still remains problematic. For the pathway, no direct detectable evidence supports the proposed retro-aldol condensation of D-glucose at the initial step. In fact, the retro-aldol condensation is more likely to be a base-catalyzed reaction,[10] and is kinetically unfavorable in the acidic vanadium(V) aqueous system. The inactive retro-aldol condensation is in conflict with the generally high rate of FA formation. Therefore, there must be another pathway to replace the retro-aldol condensation. In addition, the information on the interaction between D-glucose and the vanadium(V) catalyst and bond cleavage is insufficient, except for an observation of a valence change in the vanadium atom ($V^V \rightleftharpoons V^{IV}$ interconversion) followed by a brief explanation relying on a pre-existing well-established electron transfer–oxygen transfer mechanism.[42]

The isotope-labelling technique is a powerful tool for the detection of the mechanism of an unknown chemical process. Transformation of the $^{13}C$-labeled vanadium-catalyzed reaction has already shown a clear contribution of each carbon atom in glucose to the final products.[26] In this work, we carried out a further more in-depth investigation towards the mechanism of vanadium(V)-catalyzed oxidative C–C bond cleavage of carbohydrates by converting $^{13}C$-/D-labeled D-glucose in $NaVO_3$–$H_2SO_4$ aqueous solution with $O_2$ as an oxidant. The $NaVO_3$–$H_2SO_4$ system was employed because it produces the highest yield of FA in aqueous media, and the aqueous form of $NaVO_3$ ($VO_2^+$ species) was much more simple and representative than other vanadium(V) systems. Intermediates were detected by NMR and LC-MS techniques, and the mechanism of C–C bond cleavage was reasonably proposed. Remarkably, this study suggests a novel, successive C1–C2 bond cleavage to generate FA and the corresponding carbohydrate with one carbon atom less. This new finding will provide deeper insight into the selective C–C bond cleavage of carbohydrates and provide guidance for screening and synthesizing new highly-efficient catalyst systems for FA production.

## 2. Experimental section

### 2.1 Chemicals

D-Glucose-1-$^{13}C$ (98%), D-glucose-2-$^{13}C$ (99%), D-glucose-3-$^{13}C$ (99%), D-glucose-1-D (98%), D-glucose-2-D (98%) and D-arabinose-1-$^{13}C$ (99%) were purchased from Cambridge Isotope Laboratories (USA). Anhydrous D-(+)-glucose (99%) was purchased from Sinopharm Chemical Reagent Co., Ltd (Beijing, China). D-(−)-Arabinose (99%), D-erythrose (75% syrup), D-glyceraldehyde (99%), glycolaldehyde (dimer, 98%) and sodium metavanadate ($NaVO_3$, AR) were purchased from Aladdin Reagent Inc. (Shanghai, China). Sulfuric acid ($H_2SO_4$, 98%) was purchased from Beijing Modern Oriental Fine Chemistry Co., Ltd (Beijing, China). Oxygen ($O_2$, 99.995%) and nitrogen ($N_2$, 99.999%) were supplied by Beijing Haipu Gases Co., Ltd (Beijing, China). All reagents were of analytical grade and used without further purification.

### 2.2 Conversion of substrates

The conversion of D-glucose and D-arabinose for $^{13}C$ NMR analysis was carried out in a 25 $cm^3$ batch reactor of Hastelloy alloy (HC 276) with a magnetic stirrer. The conversion of the isotope-labeled substrates was carried out in a 1.5 $cm^3$ capped glass vial, which was equipped with a porous cap and a magnetic stirrer, fixed in the above-mentioned batch reactor. In a typical procedure, a certain amount of substrate and $NaVO_3$–$H_2SO_4$ ($H_2SO_4$, $NaVO_3$, or $NaVO_3$–$D_2SO_4$) aqueous solution were loaded into the reactor (or the glass vial). Then the reactor was sealed and purged with $O_2$ (or $N_2$). After that, $O_2$ (or $N_2$) was charged into the reactor to a desired pressure. Next, the reactor was put into a heating furnace and stirred at a speed of 500 rpm. The pressure and temperature of the reactor were measured by a pressure transducer (±0.025 MPa) and a thermocouple (±0.5 °C),

respectively. The reaction time was recorded when the desired reaction temperature was reached (~25 min after being put into the furnace). After the reaction, the reactor was quenched by cold water. When the reactor reached room temperature, the gas was released. The liquid sample was analyzed by NMR and LC-MS.

The kinetics experiments were carried out in a 50 $cm^3$ reactor of Hastelloy alloy (HC 276) with a magnetic stirrer and a liquid outlet. In a typical procedure, a certain amount of substrate and 30 $cm^3$ of $NaVO_3$–$H_2SO_4$ aqueous solution were loaded into the reactor. The operation was just the same as that of the batch reactor, except for a higher stirring speed of 900 rpm and a shorter heat-up time of 5 min. The reaction time was recorded when the desired reaction temperature was reached. The liquid sample from the outlet was collected every 30 min. The liquid sample was analyzed by liquid chromatography.

### 2.3 Analysis of the products

The yields of the products in the liquid sample were calculated using a high-performance liquid chromatograph (HPLC, Waters 2695, USA) with a Shodex SH 1011 column (Shodex, Japan). A differential refractive index detector (Waters 4110, USA) was employed to analyze the products. The column oven temperature was 55 °C. The mobile phase was diluted $H_2SO_4$ aqueous solution at a concentration of 0.01 mol $dm^{-3}$ and a flow rate of 0.5 $cm^3$ $min^{-1}$. All the yields of the products were calculated on the carbon base. The intermediates formed during the conversion were detected using LC-MS and NMR techniques. The LC part of LC-MS was a high-pressure liquid chromatography instrument (Agilent 1290 Infinity, USA) equipped with a Zorbax $NH_2$ column (Agilent, USA). The mobile phase was water/acetonitrile with gradient elution. The MS part was a micrOTOF QII mass spectrometer (Bruker Daltonics, Germany) using an electrospray ion (ESI) source in the positive mode. The $^{13}C$ NMR and $^1H$ NMR spectra of the liquid mixture were detected on a Bruker AV400 MHz spectrometer with deuterium oxide as the reaction medium. The FA formed in the conversion of glucose in $H_2{}^{18}O$ was extracted with a twofold greater volume of ethyl ether (AR). The GC-MS measurements of the extracted FA were recorded using an ISQ MS detector and a TRACE 1300 gas chromatograph equipped with a TG-WaxMS column (30 m × 0.25 mm × 0.25 μm). The carrier gas was helium.

## 3. Results and discussion

### 3.1 Initial C1–C2 bond cleavage to FA and arabinose

All the reactions of D-glucose oxidation by $O_2$ in $NaVO_3$–$H_2SO_4$ aqueous solution in this work were performed at 100 °C, lower than the applied temperatures for FA production (usually >100 °C). Under these relatively mild conditions, the D-glucose conversion rate was slowed down and more intermediates were possibly formed and preserved in the reaction mixture available for detection. The $^{13}C$ NMR spectra for the reaction mixtures indicate that an intermediate, D-arabinose, was formed and then diminished with a prolonged reaction time (Fig. 1). The $^1H$ NMR

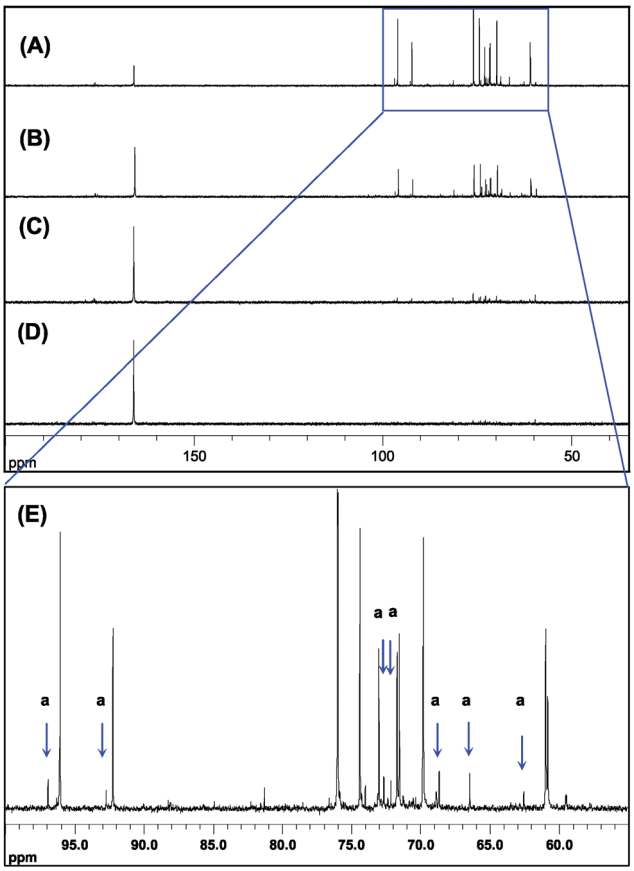


Fig. 1 $^{13}C$ NMR spectra of the reaction mixture with D-glucose as the substrate at different reaction times. (A) 2 h, (B) 4 h, (C) 8 h, (D) 12 h, and (E) the region of 55–100 ppm of (A), showing signals of D-arabinose (a). Reaction conditions: D-glucose, 1 g; $NaVO_3$, 0.35 wt%; $H_2SO_4$, 1 wt%; $H_2O$, 6 $cm^3$; initial $O_2$, 3 MPa; temperature, 100 °C.

spectrum (Fig. S1, ESI†) and the detection of $C_5H_{10}O_5Na^+$ (*m*/*z*: 173, Fig. S2, ESI†) in LC-MS of the reaction mixture provide further evidence for D-arabinose formation. Simultaneously, FA was formed and accumulated (165.80 ppm, Fig. 1).

D-Arabinose is a pentose with one carbon less than glucose. We observed that D-arabinose shares the same carbon skeleton from C2 to C5 with D-glucose (on both linkage and chirality). Therefore, we speculate that C1–C2 bond cleavage occurs in glucose oxidation to generate FA and D-arabinose (Scheme 1).

A series of $^{13}C$-labeled experiments were then carried out for further confirmation of this assumption. The $^{13}C$-labeled FA

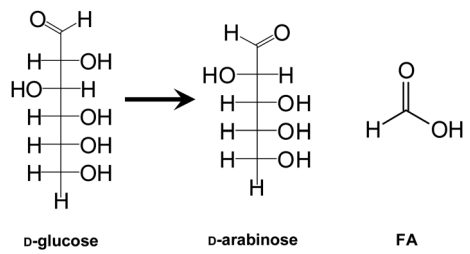


Scheme 1 D-Arabinose and FA formation from D-glucose.

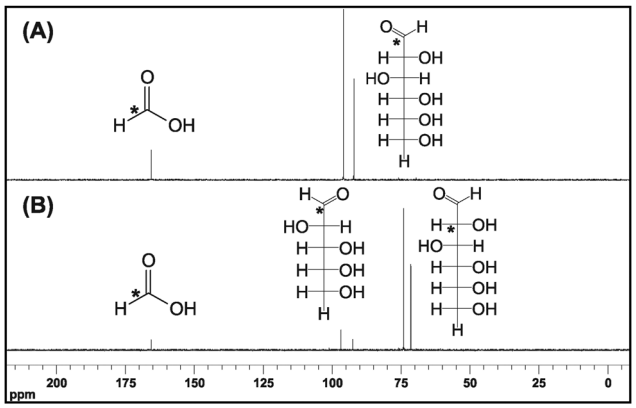


Fig. 2 $^{13}C$ NMR spectra of the reaction mixture with (A) D-glucose-1-$^{13}C$ and (B) D-glucose-2-$^{13}C$ as the substrate. Reaction conditions: D-glucose-1-$^{13}C$ or -2-$^{13}C$, 0.005 g; $NaVO_3$, 0.2 wt%; $D_2SO_4$, 1 wt%; $D_2O$, 0.5 $cm^3$; initial $O_2$, 3 MPa; temperature, 100 °C; reaction time, 10 min.

was largely formed from the short-time reaction of D-glucose-1-$^{13}C$, as detected by $^{13}C$ NMR (Fig. 2A, the $^{13}C$ assignment in $^{13}C$ NMR is listed in Table S1, ESI†). Unlabeled D-arabinose should be formed, but the intensity was too low to be observed compared with the labeled products. When D-glucose-2-$^{13}C$ was employed as the substrate under identical conditions, D-arabinose-1-$^{13}C$ was detected in the $^{13}C$ NMR spectrum with a weaker signal of $^{13}C$-labeled FA (Fig. 2B). Notably, no other labeled products were found in both spectra. These results indicate that D-glucose firstly undergoes C1–C2 bond cleavage with the C1 segment to form FA and the C2–C6 segment to form D-arabinose. Continuous C1–C2 bond cleavage can proceed (Scheme 2), as evidenced by the delayed formation of $^{13}C$–FA in D-glucose-2-$^{13}C$ conversion.

In aqueous medium, carbohydrates can undergo retro-aldol condensation, requiring cleavage of the C2–C3 bond[43,44] or the C3–C4 bond.[9] Therefore, FA generation from glucose has usually been considered to involve C2–C3 bond cleavage and/or C3–C4 bond cleavage. In the $NaVO_3$–$H_2SO_4$ catalytic system, even the $^{13}C$-labeled products with two or three carbons were not detected, and these two kinds of cleavages for FA formation cannot be entirely excluded. It is also possible that two- or three-carbon labeled products were formed followed by very quick degradation to form $^{13}C$–FA. One simple way to rule out this possibility is to measure and compare the amounts of the

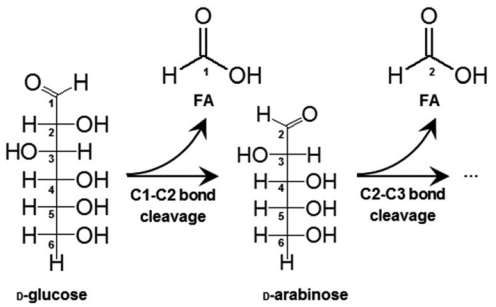


Scheme 2 Successive C1–C2 bond cleavage of D-glucose.

products at one specific reaction time. Considering that D-arabinose can soon be converted as formed, we conducted the reaction (D-glucose-1-$^{13}C$ as the substrate) in a very short time to prevent further degradation of the formed D-arabinose as much as possible. The reaction mixture was analyzed by $^1H$ NMR (Fig. 3). In the downfield of the $^1H$ NMR spectrum, the two symmetric peaks (7.85 ppm and 8.40 ppm) are assigned to aldehydic H in $^{13}C$–FA due to splitting of the H signal by the coupling effect between $^1H$ and $^{13}C$ ($^1J_{H,C}$ = 219.2 Hz). The weaker signal between the split two peaks is assigned to aldehydic H in unlabeled FA. The integration of the peaks of the H signals in $^{13}C$–FA and in H1 of D-arabinose in the α-conformation (4.35 ppm) gives the ratio of the formed $^{13}C$–FA to D-arabinose ~0.9 : 1. This result clearly shows that C1–C2 bond cleavage to generate FA is the main reaction at the initial step of the whole conversion.[45]

In contrast, experiments with no $NaVO_3$–$H_2SO_4$ or $NaVO_3$ under the same conditions show no formation of any products, suggesting a specific interaction between the catalyst and D-glucose.

### 3.2 Parallel side-reaction: epimerization of D-glucose to D-mannose with a C1–C2 shift

Interestingly, when a larger amount of $NaVO_3$–$H_2SO_4$ aqueous solution was employed, a side reaction appeared with the detection of a new labeled carbohydrate, D-mannose-2-$^{13}C$ in D-glucose-1-$^{13}C$ transformation (Fig. S3, ESI†). The reaction with D-glucose-2-$^{13}C$ under identical conditions gave a labeled D-mannose-1-$^{13}C$ (Fig. S4, ESI†). With the absence of $O_2$ supply (replacement with $N_2$), unlabeled D-glucose produces a considerable amount of D-mannose, as clearly detected from the $^{13}C$ NMR spectrum (in order to give an observable result, the reaction was carried out in one batch reactor three times by adding 0.35 wt% $NaVO_3$ each time). This result reveals that $NaVO_3$–$H_2SO_4$ catalyzes the epimerization of glucose to mannose *via* a C1–C2 shift (Scheme 3). This epimerization possibly involves an interaction of the catalyst and C3 of D-glucose, C2–C3 bond cleavage and C1–C3 bond formation.[12,46,47]

Data based on liquid chromatography have revealed that the D-mannose formation rate on D-glucose conversion is lower than the glucose formation rate on mannose conversion (Fig. S5, ESI†). Furthermore, the FA formation rate on glucose conversion is faster than that on mannose conversion. Notably, in the whole scope of the reaction time, while D-mannose-2-$^{13}C$ was formed in D-glucose-1-$^{13}C$ conversion, no D-arabinose-1-$^{13}C$ was observed (Fig. S3, ESI†). These phenomena suggest that, even though D-mannose was formed, FA was still generated primarily from D-glucose.

### 3.3 Further reactions: dimerization, deep C1–C2 bond cleavage and C–C bond reformation

We used the intermediate D-arabinose as the starting material to test the pathway of further degradation of D-glucose (Fig. S6, ESI†). D-Arabinose was converted much faster than D-glucose, as it was found to be diminished in 2 h by $^{13}C$ NMR (D-glucose in more than 8 h, as shown in Fig. 1). This can explain the low

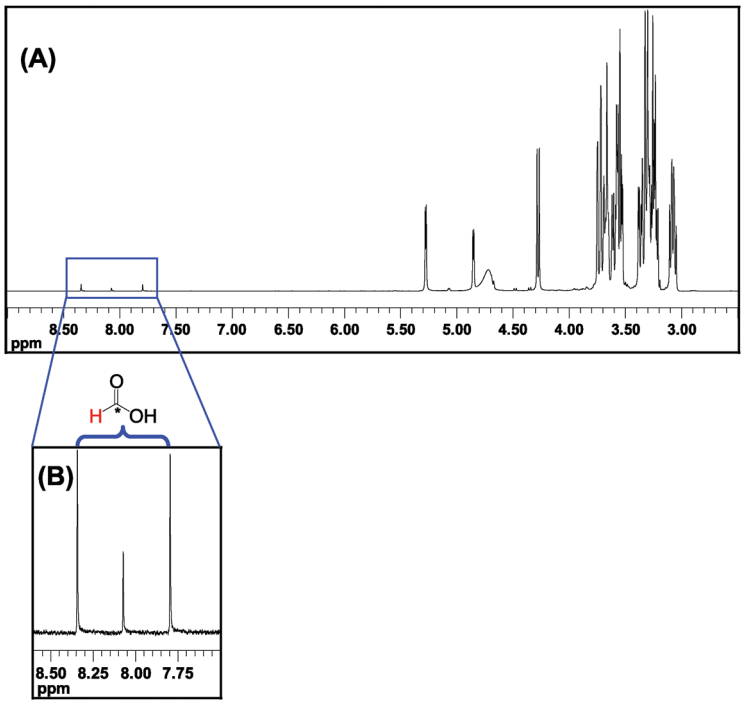


Fig. 3 $^{1}$H NMR spectra of the reaction mixture with D-glucose-1-$^{13}$C. (A) Full spectrum, and (B) the region of 7.5–8.6 ppm of (A). The central signal is attributed to H in FA, and the split signal is attributed to H in $^{13}$C–FA ($^{1}J_{H,C}$ = 219.2 Hz). Reaction conditions: D-glucose-1-$^{13}$C, 0.005 g; $NaVO_3$, 0.35 wt%; $D_2SO_4$, 1 wt%; $D_2O$, 0.5 cm$^3$; initial $O_2$, 3 MPa; temperature, 100 °C; reaction time, 0 min (the reaction was quenched as the reactor just reached the desired temperature).

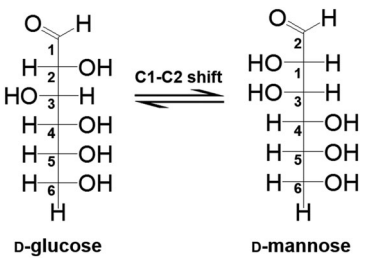


Scheme 3 Epimerization of D-glucose to D-mannose in the $NaVO_3$–$H_2SO_4$ aqueous solution with a C1–C2 shift.

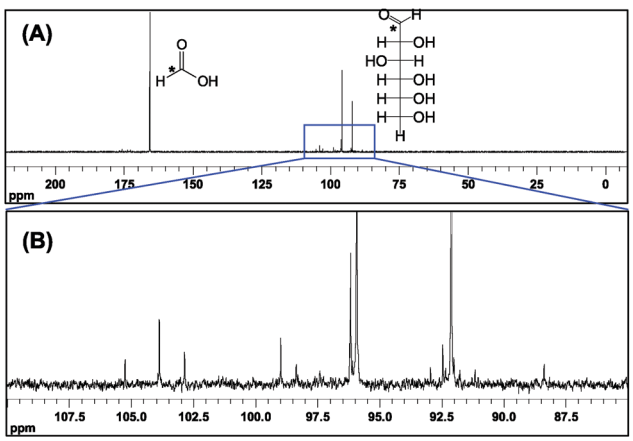


Fig. 4 $^{13}$C NMR spectra of the reaction mixture with D-glucose-1-$^{13}$C as the substrate after a prolonged reaction time. (A) Full spectrum. (B) The region of 85–110 ppm of (A). Reaction conditions: D-glucose-1-$^{13}$C, 0.005 g; $NaVO_3$, 0.2 wt%; $D_2SO_4$, 1 wt%; $D_2O$, 0.5 cm$^3$; initial $O_2$, 3 MPa; temperature, 100 °C; reaction time, 2 h.

accumulation of D-arabinose in the whole time scope of the D-glucose conversion. The potential products of C1–C2 bond cleavage of D-arabinose were indistinct in the $^{13}$C NMR spectra.

Valuable information on further reactions can be acquired according to the $^{13}$C-labelling experiments. After a longer reaction of D-glucose-1-$^{13}$C, weak signals appeared between 97 and 107 ppm in the $^{13}$C NMR spectrum (Fig. 4). These can be attributed to the C1 of disaccharides. The detection of $C_{12}H_{22}O_{11}Na^+$ (*m*/*z*: 365) in LC-MS analysis (with unlabeled D-glucose as the starting material) further gives evidence of disaccharide formation *via* the dimerization of D-glucose (Fig. S7, ESI†). These results indicate that C1–C2 bond cleavage proceeds predominantly in D-glucose degradation, accompanied by a low level of dimerization.

Besides the detection of D-arabinose-1-$^{13}$C and $^{13}$C-FA, the reaction of D-glucose-2-$^{13}$C under identical conditions provides an additional signal attributed to arabinonic acid-1-$^{13}$C (176.12 ppm) in the $^{13}$C NMR spectrum (Fig. 5). The $^{13}$C NMR spectrum of the reaction with D-arabinose-1-$^{13}$C also provides the same signal (176.18 ppm) assigned to arabinonic acid-1-$^{13}$C (Fig. 6). These indicate that besides C–C bond cleavage, C–H bond cleavage in C1 of D-arabinose has occurred. In the region of 68–78 ppm, weak signals of C2 in disaccharides were also observed.

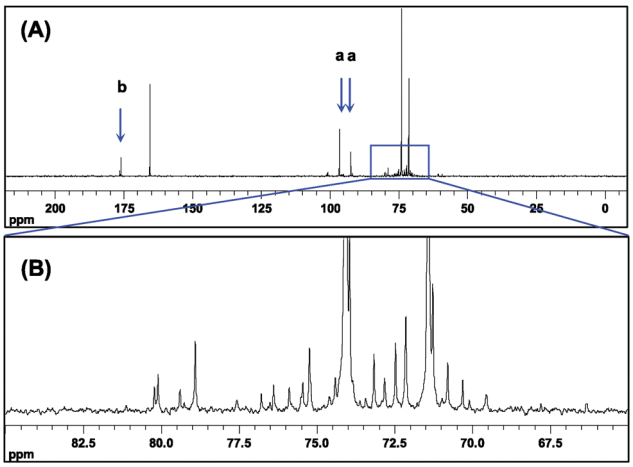


Fig. 5 $^{13}$C NMR spectra of the reaction mixture with D-glucose-2-$^{13}$C as the substrate after a prolonged reaction time. (A) Full spectrum, showing the signals of D-arabinose-1-$^{13}$C (a) and D-arabinonic acid-1-$^{13}$C (b). (B) The region of 65–85 ppm of (A). Reaction conditions: D-glucose-2-$^{13}$C, 0.005 g; $NaVO_3$, 0.2 wt%; $D_2SO_4$, 1 wt%; $D_2O$, 0.5 cm$^3$; initial $O_2$, 3 MPa; temperature, 100 °C; reaction time, 2 h.

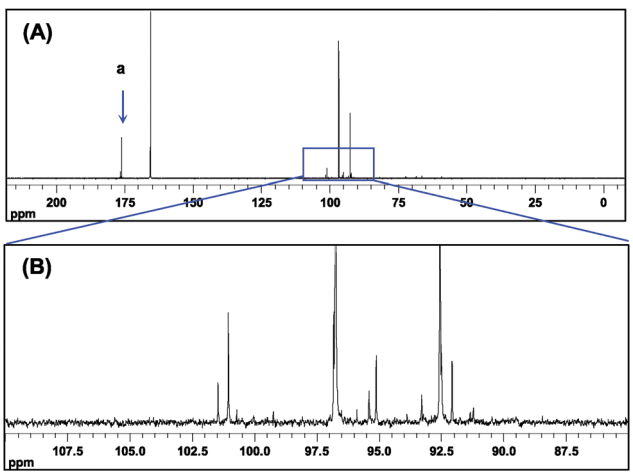


Fig. 6 $^{13}$C NMR spectra of the reaction mixture with D-arabinose-1-$^{13}$C as the substrate after a prolonged reaction time. (A) Full spectrum, showing the signal of D-arabinonic acid-1-$^{13}$C (a). (B) The region of 85–110 ppm of (A). Reaction conditions: D-arabinose-1-$^{13}$C, 0.005 g; $NaVO_3$, 0.2 wt%; $D_2SO_4$, 1 wt%; $D_2O$, 0.5 cm$^3$; initial $O_2$, 3 MPa; temperature, 100 °C; reaction time, 1 h.

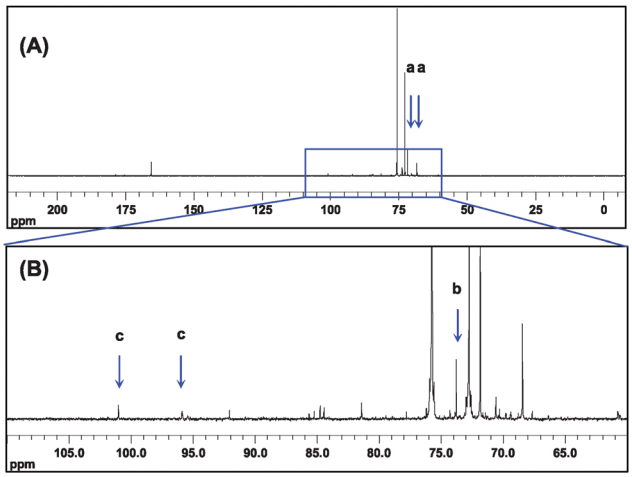


Fig. 7 $^{13}$C NMR spectra of the reaction mixture with D-glucose-3-$^{13}$C as the substrate after a prolonged reaction time. (A) Full spectrum, showing the signals of D-arabinose-2-$^{13}$C (a). (B) The region of 60–110 ppm of (A), showing the signals of D-arabinonic acid-2-$^{13}$C (b) and D-erythrose-1-$^{13}$C (c). Reaction conditions: D-glucose-3-$^{13}$C, 0.005 g; $NaVO_3$, 0.2 wt%; $D_2SO_4$, 1 wt%; $D_2O$, 0.5 cm$^3$; initial $O_2$, 3 MPa; temperature, 100 °C; reaction time, 1 h.

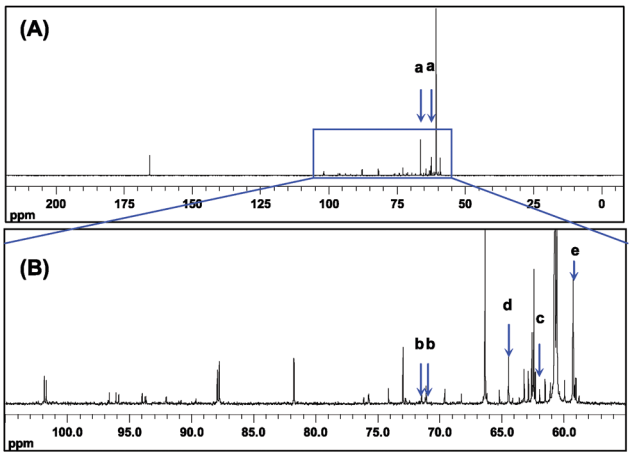


Fig. 8 $^{13}$C NMR spectra of the reaction mixture with D-glucose-6-$^{13}$C as the substrate. (A) Full spectrum, showing the signals of D-arabinose-5-$^{13}$C (a). (B) The region of 55–105 ppm of (A), showing the signals of D-erythrose-4-$^{13}$C (b), D-glyceraldehyde-3-$^{13}$C (c), glycolaldehyde-2-$^{13}$C (d) and glycolic acid-2-$^{13}$C (e). Reaction conditions: D-glucose-3-$^{13}$C, 0.005 g; $NaVO_3$, 0.2 wt%; $D_2SO_4$, 1 wt%; $D_2O$, 0.5 cm$^3$; initial $O_2$, 3 MPa; temperature, 100 °C; reaction time, 1 h.

The $^{13}$C NMR spectrum of the reaction with D-glucose-3-$^{13}$C shows the signals assigned to D-arabinose-2-$^{13}$C (Fig. 7). The signal at 73.79 ppm possibly refers to C2 in arabinonic acid, further confirming the oxidation of D-arabinose on C1.

More information on further reactions can be obtained using D-glucose-6-$^{13}$C as the substrate. C1–C2 bond cleavage leads to D-arabinose-5-$^{13}$C generation, as detected in the $^{13}$C NMR spectrum (66.36 ppm and 62.44 ppm, Fig. 8). The signals of C6 in disaccharides (~61 ppm) and C5 in arabinonic acid should be highly overlapped by the strong response of labeled C6 in D-glucose-6-$^{13}$C.

Notably, even though the intensity was weak, a tetrose, D-erythrose-4-$^{13}$C, was detected (71.47 ppm and 71.11 ppm). D-erythrose-1-$^{13}$C was also identified in the $^{13}$C NMR spectrum of the reaction with D-glucose-3-$^{13}$C (101.02 ppm and 95.87 ppm, Fig. 7). According to the experiments for either C1 or C2 labeled D-glucose, no C2–C3 bond cleavage products were formed. Thus, D-erythrose-4-$^{13}$C can only be possibly generated *via* C1–C2 bond cleavage of the formed D-arabinose-5-$^{13}$C (Scheme 4). In addition, the triose, D-glyceraldehyde-3-$^{13}$C, was also detected (62.31 ppm, Fig. 8). No significant signals of C2 or C3 products were observed in the reaction with D-arabinose-1-$^{13}$C, suggesting that D-glyceraldehyde-3-$^{13}$C is

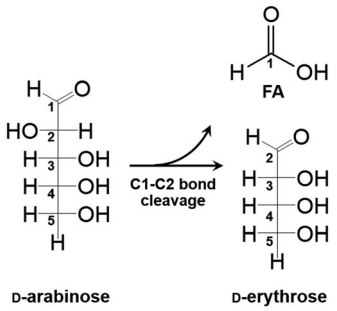


Scheme 4 C1–C2 bond cleavage of D-arabinose to D-erythrose.

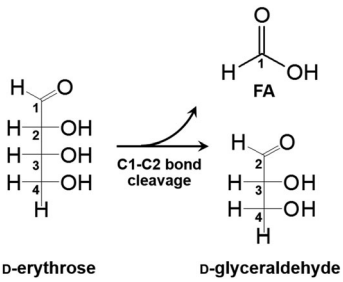


Scheme 5 C1–C2 bond cleavage of D-erythrose to D-glyceraldehyde.

mainly derived from D-erythrose-4-$^{13}$C *via* C1–C2 bond cleavage (Scheme 5). The observation of glycolaldehyde-2-$^{13}$C in the $^{13}$C NMR spectrum (64.47 ppm, Fig. 8) indicates C1–C2 bond cleavage of D-glyceraldehyde-3-$^{13}$C. In addition, the glycolic acid-2-$^{13}$C detection (59.25 ppm, Fig. 8) suggests the oxidation of the aldehyde group in glycolaldehyde-2-$^{13}$C. The dimerization can also be found between D-glucose and D-glyceraldehyde/glycolaldehyde (or between D-arabinose and D-glyceraldehyde), as evidenced by the detection of $C_9H_{16}O_8$ and $C_8H_{14}O_7$ by LC-MS (Fig. S8, ESI†).

It is also worth noting that in the D-glucose-6-$^{13}$C reaction, $^{13}$C-labeled signals appeared in the region of 68–103 ppm (Fig. 8). The signals between 68 and 85 ppm, which share a similar region of the non-terminal carbons in the aldose structure, suggest a shift of the $^{13}$C-labeled carbon from the terminal position (in D-glucose) to the non-terminal position as a form of some new types of carbohydrates. These carbohydrates can most likely be generated by C–C bond reformation between the existing terminal $^{13}$C-labeled products in the reaction mixture, probably by aldol condensation, which commonly occurs in carbohydrate aqueous solution.

Detection of substances with larger *m*/*z* values (larger than 203, which is assigned to D-glucose ($C_6H_{12}O_6Na^+$)) in LC-MS confirms the existence of aldol condensation (Fig. S8, ESI†). $C_8H_{14}O_8$ can possibly be generated *via* aldol condensation between $C_6H_{10}O_6$ (detected as $C_6H_{10}O_6Na^+$, *m*/*z*: 201) and glycolaldehyde ($C_2H_4O_2$). The reactions of three sugars (glycolaldehyde, D-glyceraldehyde and D-erythrose) and their mixtures were carried out respectively in $H_2SO_4$ solution in the absence of $NaVO_3$ and $O_2$ (replaced by $N_2$ with the same initial pressure). The $^{13}$C NMR spectrum for each shows similar signals at 68–103 ppm (Fig. S9, ESI†), indicating that the carbohydrate intermediates actually undergo acid-catalyzed aldol condensation to form longer-carbon-chain carbohydrates. Notably, the signals between 85 and 103 ppm (Fig. 8) represent the anomeric carbons of carbohydrates (that is, C1 of aldoses). This detection indicates that some regenerated 2-$^{13}$C- or 3-$^{13}$C-labeled carbohydrates were further degraded *via* C1–C2 bond cleavage, leading to the formation of 1-$^{13}$C-labeled carbohydrates. This can be evidenced by the detection of $C_7H_{12}O_7$ in LC-MS, which is possibly generated from $C_8H_{14}O_8$ *via* C1–C2 bond cleavage (Fig. S8, ESI†).

In summary, even though various intermediates were formed in glucose degradation (*via* C1–C2 bond cleavage, dimerization or aldol condensation), they largely share similar characteristics in terms of their chemical structure: most of them were assigned to carbohydrates. Given the fact that the final liquid product was solely FA, we can reasonably conclude that these carbohydrates should share exactly the same fundamental mechanism to generate FA: C1–C2 bond cleavage. Therefore, a detailed discussion about this representative C1–C2 bond cleavage of D-glucose has been made in the following section.

### 3.4 Mechanism of C1–C2 bond cleavage of glucose and FA formation

Before the mechanism was discussed, we focused on an intermediate, $C_6H_{10}O_6$, which was undetected in $^{13}$C NMR but showed signals in LC-MS (*m*/*z*: 201, $C_6H_{10}O_6Na^+$, Fig. S7, ESI†). This compound was further identified as 2-D-glucosone (C2 of D-glucose was oxidized by hydrogen abstraction) by the observation of glucosone–quinoxaline (*m*/*z*: 251, $C_{12}H_{15}O_4N_2^+$, Scheme S1, ESI†) after adding *o*-phenylenediamine to the reaction mixture. It might be plausible that 2-glucosone is the intermediate from D-glucose to D-arabinose, *via* hydrogen abstraction on C2 followed by hydrolysis to form FA and D-arabinose (a similar reaction has occurred in the degradation of 2-D-glucosone in phosphate buffer[48]). We carried out D-glucose oxidation in $D_2O$ with $NaVO_3$–$D_2SO_4$ and found that no D-labeled D-arabinose was formed (LC-MS showed only the signal of $C_5H_{10}O_5Na^+$, representing D-arabinose, Scheme S2A, ESI†). This result indicates that the hydrogen in C1 of D-arabinose is not from aqueous solution (neither $D_2SO_4$ nor $D_2O$), thus excluding 2-glucosone as the precursor.

Additionally, no exchange between H2 and any other H atom of D-glucose occurs during C1–C2 bond cleavage as proved respectively by using D-glucose-1-D and D-glucose-2-D as substrates for LC-MS analysis (Scheme S2B and C, ESI†). No D-arabinose-1-D was detected in the reaction of D-glucose-1-D, and no D-arabinose was detected in the reaction of D-glucose-2-D. The kinetic isotope effect (KIE) is not obvious at H2 of glucose ($k_{H2}/k_{D2}$ = 1.11), suggesting a low level of C2–H bond cleavage (Fig. 9). All these results indicate that no C2–H bond cleavage occurs in D-arabinose formation.

The exchange between C2 and any other C atom of the D-glucose bond cannot occur likewise, as already evidenced by $^{13}$C NMR analysis for the experiments with D-glucose-1-$^{13}$C in Section 3.1. A C1–C2 shift can occur in D-glucose epimerization

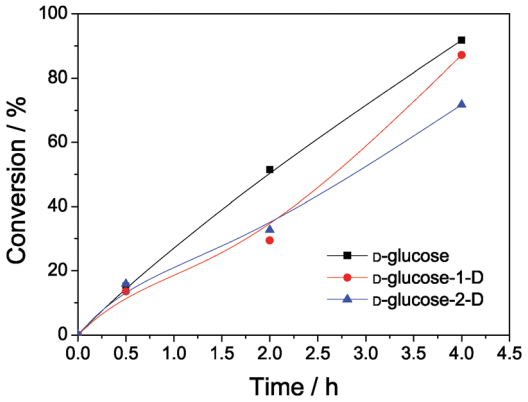


Fig. 9 The comparison of the dependence of conversion of D-glucose, D-glucose-1-D and D-glucose-2-D on the reaction time. Reaction conditions: D-glucose/D-glucose-1-D/D-glucose-2-D, 0.005 g; $NaVO_3$, 0.35 wt%; $H_2SO_4$, 1 wt%; $H_2O$, 0.5 $cm^3$; initial $O_2$, 3 MPa; temperature, 100 °C.

to D-mannose at a very low level only with an excess amount of $NaVO_3$–$H_2SO_4$, and no C–C bond cleavage was found after the shift (as discussed in Section 3.2).

After C1–C2 bond cleavage, FA was formed simultaneously with D-arabinose. At the initial step of the reaction of D-glucose-1-$^{13}$C, the obvious split signal of H1 in the $^{13}$C NMR spectrum is due to the spin-coupling of the adjacent $^{13}$C atom (as discussed in Section 3.1). This shows that the C1–H bond is reserved in FA after C1–C2 bond cleavage. The KIE of H1 is also not remarkable enough ($k_{H1}/k_{D1}$ = 1.30) to confirm the existence of C1–H bond cleavage (Fig. 9).

FA generation from D-glucose requires an extra oxygen atom. We conducted the oxidation in $^{18}$O-labeled water ($H_2{}^{18}O$) to seek the source of oxygen in FA. Two oxygen atoms were inserted into molecular FA (*m*/*z*: 50, $CH_2{}^{18}O_2$, found by GC-MS, Fig. 10). No unlabeled FA (*m*/*z*: 46, $CH_2O_2$) was detected. The result suggests that the oxygen atom in FA was potentially derived from water, probably *via* hydrated

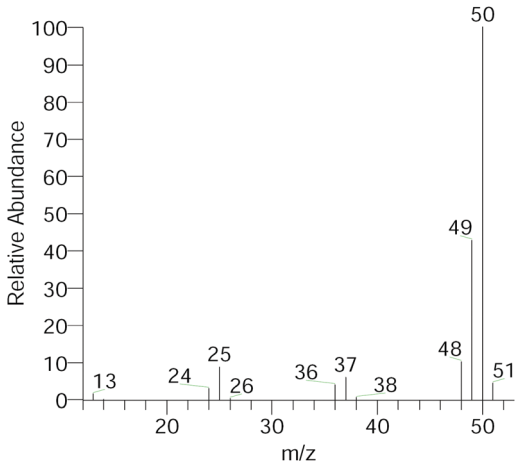


Fig. 10 Mass spectrum of FA extracted by ethyl ether after reaction under the $NaVO_3$–$H_2SO_4$ system in $H_2{}^{18}O$. Reaction conditions: D-glucose, 0.003 g; $NaVO_3$, 0.35 wt%; $H_2SO_4$, 1 wt%; $H_2{}^{18}O$, 0.2 $cm^3$; initial $O_2$, 3 MPa; temperature, 100 °C, reaction time, 1 h.

D-glucose (see below). Actually, the fact that $O_2$ was not involved in FA formation can be precisely evidenced by the experiment with D-glucose-1-$^{13}$C in the absence of $O_2$. The $^{13}$C NMR spectrum clearly shows no difference with that of the experiment with $O_2$ (FA–$^{13}$C was still detected in the spectrum, as shown in Fig. S10, ESI†). In other words, the effect of $O_2$ can only participate in the oxidation of reduced vanadium(IV) to vanadium(V).

Our previous work has confirmed that the coexistence of $NaVO_3$ and $H_2SO_4$ enhances the selectivity of FA generation from glucose by forming a high-reducibility $VO_2^+$ species under acidic aqueous solution.[30] The vanadium(V) species is reduced by the substrate to vanadium(IV) and then is re-oxidized by $O_2$. Similar mechanisms were proposed in $H_5PV_2Mo_2O_{40}$ and $VOSO_4$ aqueous systems.[19,23,29] $NaVO_3$ in the acidic aqueous solution (pH < 1) predominantly exists as a $VO_2^+$ species at room temperature.[49] This species is usually hydrolyzed in water as its hydrated form, $VO_2(H_2O)_n^+$, which lacks hydroxyl groups bonded to the vanadium atom.[50] At a higher temperature (near the reaction temperature), the $VO_2^+$ species is probably in the form of an analogue of phosphoric acid, $VO(OH)_3$, which has three hydroxyl groups bonded to one vanadium atom.[51] It is easily speculated that one possible interaction between the catalyst and D-glucose is initialized *via* the esterification of $VO(OH)_3$ and D-glucose by dehydration from both hydroxyl groups.

Various techniques including $^{13}$C/$^{51}$V NMR and LC-MS can hardly provide accurate information about the complex of a vanadium species and D-glucose. The undetectability of the complex is probably due to the readily-hydrolyzed characteristics of the vanadate in aqueous solution. However, the conclusion that C1–C2 bond cleavage occurs at the initial stage of the reaction (in Section 1) strongly suggests that the interaction site is around C1 and C2 of D-glucose.

The oxidation of D-glucose to FA is a two-electron reaction, which indicates that two equiv. of vanadium atoms are reduced from V to IV when D-glucose is oxidized to 1 equiv. of FA. Thus, we further carried out kinetic studies of glucose oxidation with the $NaVO_3$–$H_2SO_4$ system. In accordance with some kinetic studies of vanadium(V)–carbohydrate systems (that is, with no $O_2$),[52,53] the rate of glucose oxidation exhibits a first-order dependence on both $NaVO_3$ concentration and D-glucose concentration (Fig. 11, detailed information is shown in Fig. S11 and S12, ESI†). These data are consistent with a mechanism in which D-glucose is first reacted with 1 equiv. of vanadium(V) species and then the intermediate is further reacted with another equiv. of vanadium(V) species to 1 equiv. of FA and 2 equiv. of vanadium(IV) species.

Based on the above analysis, a mechanism of C1–C2 bond cleavage of D-glucose and oxidation to FA by $O_2$ under $NaVO_3$–$H_2SO_4$ aqueous solution was proposed (Scheme 6). D-Glucose is first reversibly transformed to its hydrated form with two hydroxyl groups bonded to C1. Esterification then occurs between $VO(OH)_3$ and two hydroxyl groups in C1 and C2 of D-glucose to form a five-membered ring. Electron transfer and C1–C2 bond weakening consequently proceed. Afterwards, C1–C2

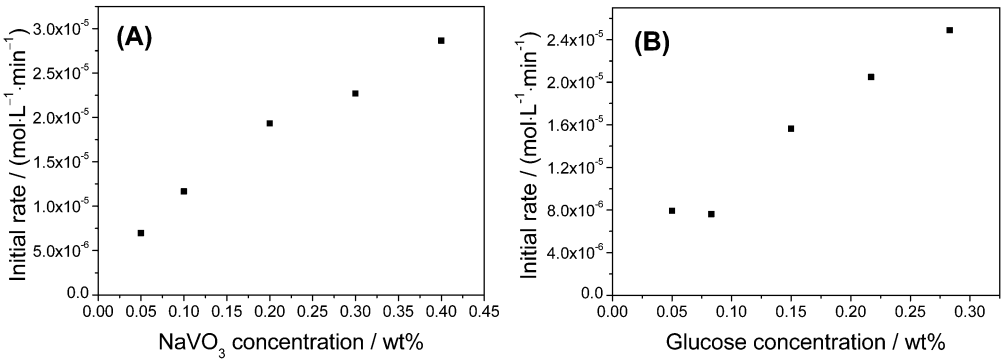


Fig. 11 Dependence of the initial rate of D-glucose conversion on (A) $NaVO_3$ concentration and (B) D-glucose concentration.

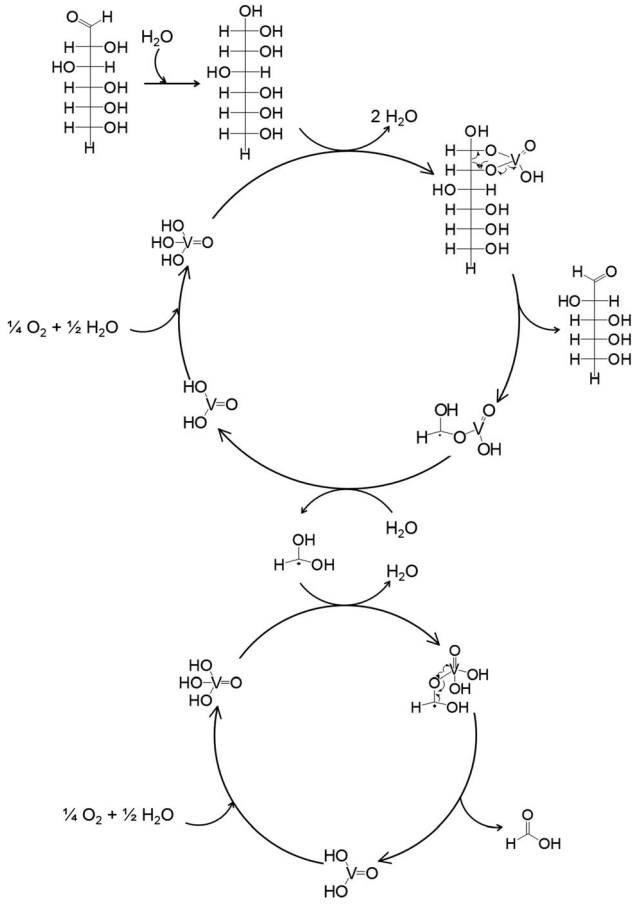


Scheme 6 The proposed mechanism of C1–C2 bond cleavage of D-glucose oxidation under $NaVO_3$–$H_2SO_4$ aqueous solution.

bond cleavage occurs, without C1/C2–H bond cleavage or a carbon skeleton rearrangement, to generate the $H_3COO^{\bullet}$–vanadium(IV) complex and arabinose. The complex is then hydrolyzed to liberate the vanadium(IV) species and free radical $H_3COO^{\bullet}$, which is rapidly oxidized by another $VO(OH)_3$ molecule to generate FA and vanadium(IV) species. The two vanadium(IV) species are then oxidized by $O_2$ to vanadium(V) species. The one-carbon-less D-arabinose and the further formed carbohydrates are degraded following a similar mechanism.

# 4. Conclusions

In this work, we studied the pathway from D-glucose to FA and the mechanism in $NaVO_3$–$H_2SO_4$ aqueous solution using isotope-labeled glucoses as substrates. D-Glucose is first transformed to FA and D-arabinose *via* C1–C2 bond cleavage. D-Arabinose undergoes a similar C1–C2 bond cleavage to form FA and the corresponding one-carbon-less D-erythrose, which can be further degraded by C1–C2 bond cleavage. The epimerization from D-glucose to D-mannose can slightly occur *via* a C1–C2 shift. Dimerization and aldol condensation between carbohydrates (either the starting material or the intermediates) can also proceed to make the reaction a much more complicated mixture. However, the fundamental reaction, C1–C2 bond cleavage, can drive all the intermediates to form the common product FA. Based on the detected intermediates, isotope-labelling experiments, KIE study and kinetic analysis, this mechanism is proposed. D-Glucose is reacted with a vanadium(V) species ($VO(OH)_3$) to form a complex with a five-membered ring. Then, electron transfer occurs and the C1–C2 bond weakens, followed by C1–C2 bond cleavage (with no C–H bond cleavage) to generate the $H_3COO^{\bullet}$–vanadium(IV) complex and arabinose. The complex is then hydrolyzed to liberate the vanadium(IV) species and free radical $H_3COO^{\bullet}$, which is rapidly oxidized by another $VO(OH)_3$ molecule to generate FA and vanadium(IV) species. The reduced vanadium species is oxidized by $O_2$ to recover to its oxidation state.

# Conflicts of interest

There are no conflicts of interest to declare.

# Acknowledgements

The authors thank Professors Zhenyu Liu and Qingya Liu for their help. This work was financially supported by the National Natural Science Foundation of China (21706007, 21676019 and 51372012), the Fundamental Research Funds for the Central Universities (ZY1601), and the long-term subsidy mechanism from the Ministry of Finance and the Ministry of Education of PRC (BUCT).

## References


1 A. Corma, S. Iborra and A. Velty, *Chem. Rev.*, 2007, **107**, 2411–2502.
2 P. Gallezot, *Chem. Soc. Rev.*, 2012, **41**, 1538–1558.
3 M. l. Besson, P. Gallezot and C. Pinel, *Chem. Rev.*, 2014, **114**, 1827–1870.
4 M. S. Holm, S. Saravanamurugan and E. Taarning, *Science*, 2010, **328**, 602–605.
5 A. Wang and T. Zhang, *Acc. Chem. Res.*, 2013, **46**, 1377–1386.
6 Y. Liu, C. Luo and H. Liu, *Angew. Chem., Int. Ed.*, 2012, **51**, 3249–3253.
7 G. Zhao, M. Zheng, J. Zhang, A. Wang and T. Zhang, *Ind. Eng. Chem. Res.*, 2013, **52**, 9566–9572.
8 X. Y. Yan, F. M. Jin, K. Tohji, T. Moriya and H. Enomoto, *J. Mater. Sci.*, 2007, **42**, 9995–9999.
9 F. Jin, Z. Zhou, T. Moriya, H. Kishida, H. Higashijima and H. Enomoto, *Environ. Sci. Technol.*, 2005, **39**, 1893–1902.
10 F. M. Jin and H. Enomoto, *Energy Environ. Sci.*, 2011, **4**, 382–397.
11 F. M. Jin, J. Yun, G. M. Li, A. Kishita, K. Tohji and H. Enomoto, *Green Chem.*, 2008, **10**, 612–615.
12 S. Caratzoulas, M. E. Davis, R. J. Gorte, R. Gounder, R. F. Lobo, V. Nikolakis, S. I. Sandler, M. A. Snyder, M. Tsapatsis and D. G. Vlachos, *J. Phys. Chem. C*, 2014, **118**, 22815–22833.
13 J. Rocek and F. H. Westheimer, *J. Am. Chem. Soc.*, 1962, **84**, 2241–2246.
14 L. Malaprade, *Bull. Soc. Chim. Fr.*, 1928, **43**, 683–690.
15 J. M. Bobbitt, *Adv. Carbohydr. Chem.*, 1956, **11**, 1–41.
16 G. Ohloff and W. Giersch, *Angew. Chem., Int. Ed.*, 1973, **12**, 401–402.
17 E. Baer, J. M. Grosheintz and H. O. L. Fischer, *J. Am. Chem. Soc.*, 1939, **61**, 2607–2609.
18 E. Amadio, R. D. Lorenzo, C. Zonta and G. Licini, *Coord. Chem. Rev.*, 2015, **301–302**, 147–162.
19 R. Wölfel, N. Taccardi, A. Bösmann and P. Wasserscheid, *Green Chem.*, 2011, **13**, 2759–2763.
20 J. Albert, R. Wölfel, A. Bosmann and P. Wasserscheid, *Energy Environ. Sci.*, 2012, **5**, 7956–7962.
21 J. Reichert, B. Brunner, A. Jess, P. Wasserscheid and J. Albert, *Energy Environ. Sci.*, 2015, **8**, 2985–2990.
22 J. Albert and P. Wasserscheid, *Green Chem.*, 2015, **17**, 5164–5171.
23 J. Li, D. J. Ding, L. Deng, Q. X. Guo and Y. Fu, *ChemSusChem*, 2012, **5**, 1313–1318.
24 J. Albert, D. Lüders, A. Bösmann, D. M. Guldi and P. Wasserscheid, *Green Chem.*, 2014, **16**, 226–237.
25 T. Lu, M. G. Niu, Y. C. Hou, W. Z. Wu, S. H. Ren and F. Yang, *Green Chem.*, 2016, **18**, 4725–4732.
26 B. B. Sarma and R. Neumann, *Nat. Commun.*, 2014, **5**, 4621.
27 J. Z. Zhang, M. Sun, X. Liu and Y. Han, *Catal. Today*, 2014, **233**, 77–82.
28 J. L. Xu, H. Y. Zhang, Y. F. Zhao, Z. Z. Yang, B. Yu, H. J. Xu and Z. M. Liu, *Green Chem.*, 2014, **16**, 4931–4935.
29 Z. Tang, W. Deng, Y. Wang, E. Zhu, X. Wan, Q. Zhang and Y. Wang, *ChemSusChem*, 2014, **7**, 1557–1567.
30 W. H. Wang, M. G. Niu, Y. C. Hou, W. Z. Wu, Z. Y. Liu, Q. Y. Liu, S. H. Ren and K. N. Marsh, *Green Chem.*, 2014, **16**, 2614–2618.
31 M. G. Niu, Y. C. Hou, S. H. Ren, W. H. Wang, Q. T. Zheng and W. Z. Wu, *Green Chem.*, 2015, **17**, 335–342.
32 M. G. Niu, Y. C. Hou, S. H. Ren, W. Z. Wu and K. N. Marsh, *Green Chem.*, 2015, **17**, 453–459.
33 A. Boddien, D. Mellmann, F. Gartner, R. Jackstell, H. Jungle, P. J. Dyson, G. Laurenczy, R. Ludwig and M. Beller, *Science*, 2011, **333**, 1733–1736.
34 Y. Himeda, *Green Chem.*, 2009, **11**, 2018–2022.
35 Z. L. Wang, J. M. Yan, Y. Ping, H. L. Wang, W. T. Zheng and Q. Jiang, *Angew. Chem., Int. Ed.*, 2013, **52**, 4406–4409.
36 T. Zell, B. Butschke, Y. Ben-David and D. Milstein, *Chem. – Eur. J.*, 2013, **19**, 8068–8072.
37 D. Mellmann, P. Sponholz, H. Junge and M. Beller, *Chem. Soc. Rev.*, 2016, **45**, 3954–3988.
38 C. Rice, S. Ha, R. I. Masel, P. Waszczuk, A. Wieckowski and T. Barnard, *J. Power Sources*, 2002, **111**, 83–89.
39 M. Weber, J. T. Wang, S. Wasmus and R. F. Savinell, *J. Electrochem. Soc.*, 1996, **143**, 158–160.
40 N. V. Rees and R. G. Compton, *J. Solid State Electrochem.*, 2011, **15**, 2095–2100.
41 Y. Nakagawa, D. Sekine, N. Obara, M. Tamura and K. Tomishige, *ChemCatChem*, 2017, **9**, 3412–3419.
42 A. M. Khenkin and R. Neumann, *J. Am. Chem. Soc.*, 2008, **130**, 14474–14476.
43 M. Sasaki, K. Goto, K. Tajima, T. Adschiric and K. Araic, *Green Chem.*, 2002, **4**, 285–287.
44 J. Zhang, B. Hou, A. Wang, Z. Li, H. Wang and T. Zhang, *AIChE J.*, 2014, **60**, 3804–3813.
45 Similar C1–C2 bond cleavage of D-glucose can be realized previously, but C1 comes to $CO_2$ *via* sequential oxidation reactions to yield α-keto-D-gluconic acid followed by decarboxylation: J. A. Stapley and J. N. BeMiller, The Ruff degradation: a review of previously proposed mechanisms with evidence that the reaction proceeds by a Hofer–Moest-type reaction, *Carbohydr. Res.*, 2007, **342**, 407–418.
46 I. Delidovich and R. Palkovits, *ChemSusChem*, 2016, **9**, 547–561.
47 M. L. Hayes, N. J. Pennings, A. S. Serianni and R. Barker, *J. Am. Chem. Soc.*, 1982, **104**, 6764–6769.
48 W. Zhang and A. S. Serianni, *J. Am. Chem. Soc.*, 2012, **134**, 11511–11524.
49 D. C. Crans, J. J. Smee, E. Gaidamauskas and L. Yang, *Chem. Rev.*, 2004, **104**, 849–902.
50 O. Bortolini and V. Conte, *J. Inorg. Biochem.*, 2005, **99**, 1549–1557.
51 A. Sadoc, S. Messaoudi, E. Furet, R. Gautier, E. L. Fur, L. l. Pollès and J.-Y. Pivan, *Inorg. Chem.*, 2007, **46**, 4835–4843.
52 K. K. S. Gupta and S. Basu, *Carbohydr. Res.*, 1979, **72**, 139–149.
53 S. C. Pati and M. Panda, *Int. J. Chem. Kinet.*, 1979, **11**, 731–740.


 